$\pi^- p$ Elastic Scattering at 2.29 GeV/c*

S. Hagopian† and V. Hagopian†
Department of Physics, Florida State University, Tallahassee, Florida 32306

and

E. Bogart,‡ R. O'Donnell,§ and W. Selove
Department of Physics, University of Pennsylvania, Philadelphia, Pennsylvania 19104
(Received 17 November 1971)

The reaction $\pi^- + p \to \pi^- + p$ has been studied in the 15-in. bubble chamber at the Princeton-Pennsylvania Accelerator. The elastic scattering cross section was determined to be 8.5 $\pm$ 0.2 mb. The forward peak fits to an exponential in t with a slope of 8.1 $\pm$ 0.2 (GeV/c)$^{-2}$. The forward differential cross section $d\sigma/d\Omega\,(0) = 17.9 \pm 0.7$ mb/sr. A fit of the center-of-mass angular distribution to Legendre polynomials needed terms up to the 12th order, corresponding to the highest nonzero partial wave of $L = 6$.

I. INTRODUCTION

The elastic events in this experiment were part of a high-resolution large-statistics bubble-chamber experiment. Other aspects of this experiment have previously been reported.[1] There exist several other measurements[2,3] of $\pi^- p$ elastic scattering near this momentum of 2.29 GeV/c, but this experiment has the largest number of events (12 675 events corresponding to 0.555 μb/event) which have minimum biases. It is not possible to determine phase shifts directly from this experiment alone, since polarization information is unavailable. A fit of the differential cross section to Legendre polynomials needed terms up to the 12th order, implying nonzero phase shifts of up to $I_{11/2}$ and $I_{13/2}$. In this paper we will discuss the details of the experiment and also our fits of the angular distributions to Legendre polynomials.

II. EXPERIMENTAL DETAILS

The 15-in. hydrogen bubble chamber at the Princeton-Pennsylvania Accelerator was exposed to a 2.29-GeV/c beam.[4] The π^- beam was fairly pure, with a small μ^- contaminant of less than 3%. This contamination was computed by two methods with consistent results. The first method calculated the fraction of μ^-'s from π^- decays compared with π^- mesons that entered the bubble chamber, using the properties of the beam optics. The result was 3%. The second method utilized the commonly called "beam counting" technique. Briefly, this procedure calculates the total cross section by counting the number of beam particles that interact in a known liquid-hydrogen path length (in g/cm^2). The difference between this cross section and the accepted value[5] was attributed to μ^- and e^-. The result was that the contamination was less than 3%.

The beam momentum spread was $\Delta p/p \approx 0.3\%$. This was also determined by two methods. The first method calculated $\Delta p/p = 0.3\%$ by measuring the spread of the beam at the second momentum focus and using properties of the beam optics. The second method utilized the 4-constraint elastic events in the bubble chamber. After determining the magnetic field of the chamber to 0.1% by matching the measured mass of $K^0 \to \pi^+\pi^-$ to the accepted value, the elastic events were reconstructed, leaving the beam momentum unknown. The results were that average $p = 2.29$ GeV/c and $\Delta p = 7$ MeV/c.

The bubble chamber was operated in a triggered mode, with a photograph taken only when an incoming π^- meson interacted somewhere in the chamber, including the entrance and exit windows of the chamber. The triggering signal was supplied by four counters arranged as follows. Two counters were placed in the beam line 4.1 and 11.4 m in front of the chamber. A coincidence between these two counters, using fast electronics, signified a beam particle. The average time spacing between beam particles was about 5 μsec, which is easily resolved by modern electronics. Two more counters placed 1.2 and 3.3 m behind the chamber intercepted the noninteracting beam particles that went through the chamber. A lack of coincidence in the two rear counters together with a coincidence of the front two counters signified that a beam track interacted somewhere in the chamber including the chamber entrance and exit windows; this triggered the picture taking mechanism of the bubble chamber and a photograph was taken. Since only events with a vertex in the fiducial volume (20 cm of liquid hydrogen) were useful and measured, it is important that the chamber windows be thin. In our experiment about half the events were useless because they came from interactions in the windows. The momentum and angle measurements of the emerging beam particles by the rear counters were so good that the biases were quite small and completely masked by scanning biases. Two separate tests were conducted to ensure that the selective triggering mode did not cause any unknown biases. About 10% of the photographs were taken without selective triggering. The various angular distributions and other distributions of events from this subsample were the same within statistical errors when compared with the rest of the events, implying no new biases. The second test used events from this nonselective sample and by the help of a computer program followed each secondary track out of the chamber. Out of a sample of 960 secondary tracks not a single one made it through both rear counters, again implying that biases are nonexistent. For this purpose the magnetic field including the fringe field was well measured. The only secondary tracks that can trigger the two rear counters are beam particles which have interacted elastically, but with a very small change in momentum and direction. A calculation for these events yields a maximum recoil proton momentum of 60 MeV/c. Since the smallest recoil proton momentum that can be observed by a human scanner in a bubble chamber is 80 MeV/c (1.5 mm in the chamber), the bias created by the triggering mechanism is completely masked by the human scanning bias, which is discussed later. No other biases were observed, such as differences in azimuthal distribution of secondary tracks. More details are given elsewhere.[4]

About 2 500 000 pulses were used, resulting in 700 000 useful pictures with a maximum of 4 beam tracks allowed per picture. Approximately 50 000 two-prong events were measured, using the University of Pennsylvania Flying Spot Digitizer (Hough-Powell Device, or HPD). The events were processed through the University of Pennsylvania Automatic Track Following (ATF) computer program using minimum guidance, i.e., the film was prescanned and the vertex of each event predigitized in two views. About 8% of the events failed the semiautomatic system. These failing events were remeasured by conventional measuring devices. The total number of measured events which were identified as elastically scattered was 12 675 events. After detailed comparison of several hundred events measured both conventionally and by the HPD, it was concluded that the HPD created neither biases nor distortions.

Most of the photographs were scanned once. About 10% of the film was rescanned. The average single-scan efficiency, assuming only random inefficiencies, was 93%. In addition there was a bias in the detection of short tracks, mostly protons. These events correspond to small-angle elastic scattering. The magnitude of this bias will be discussed in Sec. III.

The vast majority of the elastic-scattering events having all tracks visible and measurable were uniquely identified by the 4-constraint kinematical fit. From the analysis of the $\pi^- + p \to \pi^- + \pi^+ + n$ reported previously,[1] where the width of the $\pi^+\pi^-$ ($\rho\omega$) interference is less than 10 MeV, we can say that the accuracy of the measurements is extremely good. The estimate of misidentified elastic events is less than a few percent.

III. FORWARD DIFFERENTIAL AND TOTAL ELASTIC CROSS SECTIONS

The determination of the total cross section is dependent on the knowledge of the experimental biases. Figure 1 shows the differential cross section $d\sigma/dt$ vs t (the four-momentum transfer squared) for small t [i.e., $-t < 0.5$ (GeV/c)^2]. The data were fitted to an exponential in t for the range $0.1 < -t < 0.4$ (GeV/c)^2. The slope of the curve was computed to be 8.1 ± 0.2 (GeV/c)$^{-2}$. It is clear that there is an experimental bias for events with $-t < 0.05$ (GeV/c)^2 (i.e., cosine of the c.m. scattering angle >0.97). This corresponds to a proton recoil momentum of about 200 MeV/c, with practically no events observed below 100 MeV/c. Using the exponential form of the forward scattering peak, the number of missed events was determined to be 2575 ± 300 events. By normalizing our total corrected number of events to a total cross section of 35.0 ± 0.3 mb as

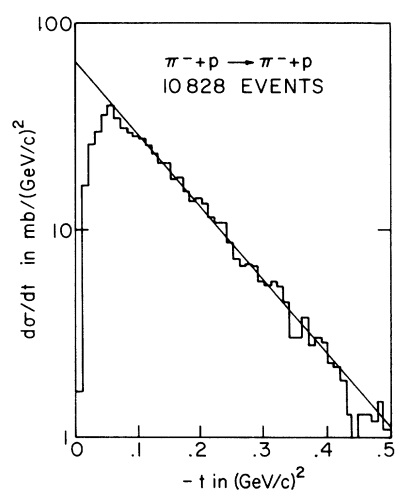

FIG. 1. $d\sigma/dt$ vs t for $\pi^- p \to \pi^- p$ with $-t < 0.5$ (GeV/c)^2, 10 828 events. Straight-line fit is for $0.1 < -t < 0.4$ (GeV/c)^2 with a slope of 8.1 ± 0.2 (GeV/c)$^{-2}$.

TABLE I. Partial cross sections at 2.29 GeV/c.

Final state	Cross section (mb)
$\pi^- + p \to \pi^- + p$	8.5 ± 0.2
$\to \pi^- + p + \pi^0$	3.8 ± 0.1
$\to \pi^- + \pi^+ + n$	4.60 ± 0.05
$\to \pi^- + p + m\pi^0$, $m \geq 2$	3.0 ± 0.1
$\to \pi^- + \pi^+ + n + m\pi^0$, $m \geq 1$	7.0 ± 0.1
$\to$ 4 charged particles	3.58 ± 0.06
$\to$ all others	4.5 ± 0.2
Total	35.0 ± 0.3

determined by a total cross-section counter experiment,[5] the elastic cross section was determined to be 8.5 ± 0.2 mb. The error is mostly due to the uncertainty in the number of the missed elastic events with small proton recoil momentum. Table I lists the cross sections for other channels from this same experiment. Work is in progress on several of the other channels.

The differential cross section at forward angle, i.e., $\theta_{\mathrm{c.m.}} = 0°$, is related to the forward scattering amplitude by

$$\frac{d\sigma}{d\Omega}(0) = |\mathrm{Im} f(0)|^2 + |\mathrm{Re} f(0)|^2 . \tag{1}$$

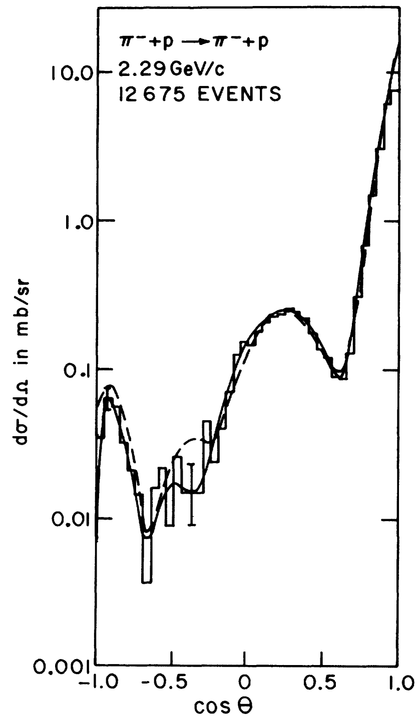

FIG. 2. $d\sigma/d\Omega$ vs $\cos\theta$ where θ is c.m. scattering angle, 12 675 events. Solid curve is a fit to the coefficients of the Legendre polynomial listed in Table III. Dashed curve is the distribution computed from the partial-wave amplitudes listed in Table IV, with no adjustable normalization parameters.

TABLE II. Number of observed events and corrected cross sections versus $\cos\theta$ where θ is c.m. scattering angle. The bias correction is only in the last bin corresponding to 2575 ± 300 events.

$\cos\theta$	Number of events	$d\sigma/d\Omega$ mb/sr	$\cos\theta$	Number of events	$d\sigma/d\Omega$ mb/sr
−1.00 to −0.95	19	0.034	0.00 to 0.05	80	0.142
−0.95 to −0.90	35	0.062	0.05 to 0.10	102	0.181
−0.90 to −0.85	31	0.055	0.10 to 0.15	115	0.204
−0.85 to −0.80	19	0.034	0.15 to 0.20	123	0.218
−0.80 to −0.75	12	0.021	0.20 to 0.25	119	0.211
−0.75 to −0.70	8	0.014	0.25 to 0.30	142	0.251
−0.70 to −0.65	2	0.004	0.30 to 0.35	137	0.242
−0.65 to −0.60	9	0.016	0.35 to 0.40	123	0.218
−0.60 to −0.55	12	0.021	0.40 to 0.45	98	0.173
−0.55 to −0.50	5	0.009	0.45 to 0.50	76	0.134
−0.50 to −0.45	14	0.025	0.50 to 0.55	70	0.124
−0.45 to −0.40	8	0.014	0.55 to 0.60	50	0.089
−0.40 to −0.35	8	0.014	0.60 to 0.65	49	0.087
−0.35 to −0.30	8	0.014	0.65 to 0.70	72	0.127
−0.30 to −0.25	25	0.044	0.70 to 0.75	171	0.303
−0.25 to −0.20	13	0.023	0.75 to 0.80	385	0.681
−0.20 to −0.15	22	0.039	0.80 to 0.85	835	1.478
−0.15 to −0.10	40	0.071	0.85 to 0.90	1750	3.098
−0.10 to −0.05	70	0.124	0.90 to 0.95	3473	6.147
−0.05 to −0.00	84	0.149	0.95 to 1.00	4258	12.095

TABLE III. Coefficients of a Legendre polynomial fit with a maximum order $n=12$. The fit is to the corrected differential cross sections presented in Table II. Also for comparison values for 2.27 GeV/c data are given (Ref. 3).

	2.27 GeV/c	2.29 GeV/c
a_0	1.45± 0.07	1.51± 0.03
a_1	3.58± 0.20	3.83± 0.09
a_2	4.97± 0.31	5.21± 0.14
a_3	5.64± 0.39	5.87± 0.19
a_4	6.03± 0.44	6.05± 0.22
a_5	5.29± 0.46	5.24± 0.24
a_6	4.00± 0.45	3.75± 0.24
a_7	2.76± 0.41	2.40± 0.22
a_8	1.88± 0.36	1.42± 0.20
a_9	1.44± 0.30	0.87± 0.16
a_{10}	0.80± 0.24	0.38± 0.12
a_{11}	0.46± 0.18	0.16± 0.08
a_{12}	0.31± 0.14	0.07± 0.04
a_{13}	0.25± 0.09	

The imaginary part of $f(0)$ is related to the total cross section (σ) through the optical theorem $\mathrm{Im} f(0)=\sigma k/4\pi$, where $k=P_{\mathrm{c.m.}}/\hbar c$. For our experiment $|\mathrm{Im} f(0)|^2=17.7\pm0.3$ mb/sr, while $d\sigma/d\Omega(0)$ determined from the data shown in Fig. 1 is 17.9 ± 0.7 mb/sr. Therefore $|\mathrm{Re} f(0)|^2=0.2\pm0.8$ mb/sr. This is completely consistent with a small real value of the forward scattering amplitude. Predictions of $|\mathrm{Re} f(0)|^2$ using dispersion-relation calculations yield[6] $|\mathrm{Re} f(0)|^2=0.4$ mb/sr in complete agreement with these data.

IV. ANALYSIS OF THE ANGULAR DISTRIBUTION

There has been some recent interest in the analysis of differential cross sections of elastic events, especially with polarized hydrogen targets[3] as a means of determining the phase shifts. Since we do not have polarization information our data alone cannot determine the phase shifts unambiguously. Figure 2 shows the differential cross section as a function of the cosine of the center-of-mass scattering angle. Table II lists the number of events and the corrected cross sections. These data have been fitted to a Legendre polynomial series of the form

$$\frac{d\sigma}{d(\cos\theta)}=2\pi\lambda\!\!\!^{-2}\sum_{l=0}^{N} a_l P_l(\cos\theta)\,. \tag{2}$$

Table III lists the values of a_l determined. In order to determine the effect of the bias corrections, which involve only the bin with $\cos\theta>0.95$, the polynomial was fitted separately with and without using the bin with $\cos\theta>0.95$. The values of the coefficients changed less than $\frac{1}{3}$ of the quoted errors. The quoted values are the results of the fit

TABLE IV. The partial-wave amplitudes for 2.29 GeV/c $\pi^- p$ elastic scattering from Ref. 3, where $ka=[\eta_l^{\pm}\exp(2i\delta_l^{\pm})-1]/2i$.

Partial wave	Reka	Imka
$S(\frac{1}{2}^-)$	0.00	0.57
$P(\frac{1}{2}^+)$	0.09	0.33
$D(\frac{3}{2}^-)$	0.032	0.24
$P(\frac{3}{2}^+)$	0.00	0.39
$D(\frac{5}{2}^-)$	0.00	0.20
$F(\frac{5}{2}^+)$	−0.035	0.19
$G(\frac{7}{2}^-)$	−0.05	0.26
$F(\frac{7}{2}^+)$	−0.04	0.12
$G(\frac{9}{2}^-)$	−0.04	0.065
$H(\frac{9}{2}^+)$	−0.01	0.10
$I(\frac{11}{2}^-)$	0.00	0.015
$H(\frac{11}{2}^+)$	0.00	0.08
$I(\frac{13}{2}^-)$	−0.01	0.01

using all the corrected data shown in Table II. To fit the data properly only terms up to $l=12$ were found to be necessary. The solid curve in Fig. 2 corresponds to the a_l values listed in Table III. N(maximum l) = 12 corresponds to the highest partial waves with $L=6$ or $I(\frac{11}{2}^-)$ and $I(\frac{13}{2}^-)$. Using partial-wave amplitudes obtained from Ref. 3 for our energy with maximum $L=6$ shown in Table IV, we calculated the expected angular distribution. The dashed curve in Fig. 2 shows this result. The agreement of the unnormalized curve with our data is very good especially in the forward peak and the secondary maximum centered around $\cos\theta=0.25$. The agreement is not quite as good in the backward direction. The backward hemisphere is much more sensitive to the detailed values of the partial-wave amplitudes, so the values listed in Table IV are probably slightly in error. The data in the backward direction can also be fitted with resonances in the direct channel only. A successful fit to previously existing data from 2 to 3 GeV/c

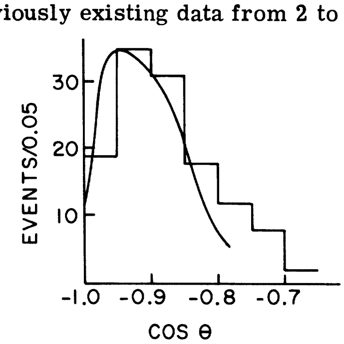

FIG. 3. $d\sigma/d\Omega$ vs $\cos\theta<-0.7$. The curve is calculated from Ref. 6 with no normalization parameters.

was made by Crittenden *et al.*[7] using known resonances in the πp system and their Regge recurrences up to 1860 MeV. The curve in Fig. 3 is the result of calculation at 2.28 GeV/c using the model of Ref. 6. The curve is not normalized to our data and the agreement is excellent.

ACKNOWLEDGMENTS

We wish to thank Dr. Y. L. Pan for his valuable assistance throughout the experiment. We would especially like to thank Professor J. D. Kimel for his help in the calculations. We would like to acknowledge helpful discussions with Professor P. K. Williams and J. Lannutti. We are grateful for the support of the staff of the Princeton-Pennsylvania Accelerator and Bubble Chamber. Also our thanks to the staffs of the University of Pennsylvania Hough-Powell Device and the high-energy computing center.

---

*Work supported in part by the U. S. Atomic Energy Commission.

†Before 1970 at University of Pennsylvania, Philadelphia, Pennsylvania.

‡Present address: Department of Radiology, University of Pennsylvania, Philadelphia, Pennsylvania.

§Present address: Mitre Corporation, Bedford, Massachusetts.

[1]S. Hagopian *et al.*, Phys. Rev. Letters 24, 1445 (1970); 25, 1050 (1970).

[2]B. G. Reynolds *et al.*, Phys. Rev. 173, 1403 (1968).

[3]R. E. Hill *et al.*, Phys. Rev. D 1, 729 (1970). Other relevant references are found in this paper.

[4]More information on this experiment can be obtained from theses of S. Hagopian and R. O'Donnell, University of Pennsylvania, 1970 (unpublished).

[5]A. Diddens *et al.*, Phys. Rev. Letters 10, 262 (1963).

[6]G. Höhler, G. Ebel, and J. Giesecke, Z. Physik 180, 430 (1964).

[7]R. R. Crittenden *et al.*, Phys. Rev. D 1, 3050 (1970), based on a model by R. R. Crittenden *et al.*, *ibid.* 1, 169 (1970). For other backward scattering data see also A. S. Carroll *et al.*, Phys. Rev. Letters 20, 607 (1968); S. W. Kormanyos *et al.*, *ibid.* 16, 709 (1966).

PHYSICAL REVIEW D VOLUME 5, NUMBER 11 1 JUNE 1972

Investigation of Low-Mass $K\pi\pi$ Systems in 12-GeV/c K^+p Interactions*

Philip J. Davis, Margaret Alston-Garnjost, Angela Barbaro-Galtieri, Stanley M. Flatté, Jerome H. Friedman, Gerald R. Lynch, Monroe S. Rabin, and Frank T. Solmitz

Lawrence Berkeley Laboratory, University of California, Berkeley, California 94720

(Received 10 December 1971)

We have studied the broad $K\pi\pi$ mass enhancements at 1300 MeV in the reactions $K^+p \to pK^+\pi^-\pi^+$ and $pK^0\pi^0\pi^+$ at 12 GeV/c. Our data were obtained from a 600 000-picture exposure of the SLAC 82-in. hydrogen bubble chamber (which corresponds to a path length of 35 events/μb). We observe a two-peak substructure in the $K^0\pi^0\pi^+$ mass spectrum at 1260 and 1420 MeV. Our estimated contribution of the $K_N(1420)$ accounts for only about half of the 1420-MeV peak (a discrepancy of about 2.4 standard deviations). The $K^+\pi^-\pi^+$ mass spectrum has a different shape. Further, assuming the $K\pi\pi$ system to be S wave 1^+ $K_V(890)\pi$ and $\rho(765)K$, we have fitted separately the $K^+\pi^-\pi^+$ and the $K^0\pi^0\pi^+$ Dalitz plots. We obtain inconsistent fits. This inconsistency and the differences in the $K\pi\pi$ mass spectra could be explained by an additional contribution of an $I=0$ S-wave $\pi\pi$ state in $K^+\pi^-\pi^+$. The $K\pi\pi$ angular decay distributions imply the dominance of the spin-parity state 1^+ with $M_z=0$ along the incident beam direction. However, there are other J^P states and states with $M_z \neq 0$. The 1260-MeV $K\pi\pi$ mass region is produced more peripherally than the 1420-MeV region.

I. INTRODUCTION

A. Purpose and Scope

The $K\pi\pi$ 1.3-GeV mass region, the Q, has been extensively studied.[1-29] (See Ref. 1 for a compilation.) Despite this effort, questions of the existence and/or nature of Q substructure remain unsettled. Interest in Q substructure is due in part to the possible assignments of two resonances to SU(3) nonets with $J^{PC}=1^{+\pm}$. In the hope of obtaining additional results regarding Q substructure, we analyze the 12-GeV/c K^+p reactions: